

The **next generation** GBCA  
from Guerbet is here

Explore new possibilities >

Guerbet | 

© Guerbet 2024 GUOB220151-A

# AJNR

## **Radiation Exposure of Patients in Comprehensive Computed Tomography of the Head in Acute Stroke**

M. Cohnen, H.-J. Wittsack, S. Assadi, K. Muskalla, A.  
Ringelstein, L.W. Poll, A. Saleh and U. Mödder

This information is current as  
of March 20, 2024.

*AJNR Am J Neuroradiol* 2006, 27 (8) 1741-1745  
<http://www.ajnr.org/content/27/8/1741>

ORIGINAL  
RESEARCH

M. Cohnen  
H.-J. Wittsack  
S. Assadi  
K. Muskalla  
A. Ringelstein  
L.W. Poll  
A. Saleh  
U. Mödder

# Radiation Exposure of Patients in Comprehensive Computed Tomography of the Head in Acute Stroke

**BACKGROUND AND PURPOSE:** To assess patient radiation exposure in comprehensive stroke imaging using multidetector row CT (MDCT) combining standard CT of the head, cerebral perfusion (CTP), and CT angiography (CTA) studies.

**METHODS:** Examination protocols for CT and CTA of cerebral and cervical vessels, as well as CTP were simulated using a Somatom Sensation Cardiac 64. Effective doses were derived from measurements with the use of lithium-fluoride thermoluminescent dosimeters (LiF-TLD) at several organ sites using an Alderson-Rando phantom.

**RESULTS:** LiF-TLD measurements resulted in effective doses of 1.7 mSv for CT, 1.9 mSv for CTA of intracranial vessels, and 2.8 mSv for CTA of cervical vessels, respectively. Depending on examination parameters, effective doses varied between 1.1 and 5.0 mSv for cerebral CTP. For CTP, local doses in the area of the primary beam ranged between 114 and 444 mGy.

**CONCLUSIONS:** Comprehensive stroke imaging may result in up to 9.5 mSv with possible local doses of 490 mGy. Although critical doses for organ damage (eg, cataract formation or hair loss) are not reached, physicians need to be aware of possible radiation induced sequelae particularly in repetitive examinations.

Imaging of patients with acute stroke evaluating cerebral perfusion using MR imaging has been widely accepted, because the mismatch concept based on the combination of diffusion and perfusion studies indicates a possible penumbra zone.<sup>1</sup> However, this demanding technology has limited accessibility and implies several contraindications, such as implanted cardiac pacemakers.<sup>2</sup>

On the other hand, CT is a widespread technique with fast image acquisition. This is particularly true for multidetector row CT systems (MDCT) and can be highly important, especially in view of the time dependent therapy concepts in acute stroke.<sup>3</sup> First data of MDCT of the head combined with perfusion CT (CTP) as well as CT angiographic (CTA) assessment of intracerebral or cervical vessels show promising results for the initial work-up of patients with acute ischemic stroke.<sup>3,4</sup>

To assess cerebral perfusion, the first pass of intravenously administered nonionic contrast agent is monitored using several continuous images acquired without changing the table position.<sup>5</sup> That is, a definite number of CT scans is performed during a limited span of time, usually between 40 and 60 seconds. To our knowledge, there are few data about the patient's radiation exposure in comprehensive MDCT stroke imaging.<sup>6,7</sup> First reports, however, have shown possible adverse effects of CTP of the brain.<sup>8</sup> Therefore, the purpose of this phantom study was to evaluate local and effective doses in 64-detector row CT of the head, including CTA and CTP studies as performed in the setting of acute stroke.

## Materials and Methods

Dose measurements were performed at a 64-detector-row CT scanner (Somatom Sensation Cardiac 64; Siemens Medical Solutions, Erlangen, Germany). We examined 4 different protocols, including a standard CT of the head and CTA of intracranial and cervical vessels. Furthermore, CTP was performed as implemented by the vendor (protocol I). Because different technical parameters are specified in literature, this protocol (270 mAs, 80 kV) was changed, and protocols II (200 mAs, 80 kV) and III (200 mAs, 120 kV) were assessed. Detailed technical parameters of all different CT examinations are given in Table 1.

After acquisition of a digital projection radiograph ("topogram") in lateral projection, the scans were planned manually according to clinical standards with a gantry angulation along the supraorbitomeatal line for the standard CT as well as the CTP protocols. CTP scans were simulated approximately at basal ganglia level. As in routine procedures, both protocols were performed in a sequential mode. (Fig 1).

The 2 CTA protocols were performed in spiral mode without gantry angulation at a detector collimation of  $64 \times 0.6$  mm. Intracranial CTA covered the internal carotid artery from the carotid bifurcation, including the complete brain as well as the venous sinuses. Therefore, phantom scanning started from the middle of the neck (approximately C5) reaching to the vertex. CTA of cervical vessels included the complete course of the carotid artery from the aortic arch (approximately C5) to the circle of Willis, which was assumed to be included if scanning reached above the temporal bone (Fig 1).

An Alderson-Rando anthropomorphic phantom (Phantom Laboratory, Salem, NY) with lithium-fluoride-thermoluminescent dosimeter (LiF-TLD-) rods ( $1 \times 6$  mm) was used to assess radiation exposure.<sup>9</sup> The TLDs had been precalibrated in absorbed dose by X-ray-irradiation under similar beam quality (0.95 mGy/nC at 100 kV, RT100). Radiation doses were assessed by reading out LiF-TLD using a Glowcurve analyzer Harshaw filtrol 2000D (Harshaw, Cleveland, Ohio) within 24 hours after exposure according to the manufacturer's information so that fading was nearly avoided.

Received September 29, 2005; accepted after revision December 8.

Institute of Diagnostic Radiology (M.C., H.-J.W., S.A., A.R., L.W.P., A.S., U.M.) and Department of Radiation Oncology (K.M.), University Hospital Düsseldorf, Düsseldorf, Germany.

Address correspondence to Priv.-Doz. Dr. M. Cohnen, Institute of Diagnostic Radiology, University Hospital, MNR-Klinik, Heinrich-Heine-University, Moorenstr. 5, 40225 Düsseldorf, Germany; e-mail: cohnem@med.uni-duesseldorf.de

**Table 1: Parameters of different scan protocols**

	Standards CT		CT Angiography		CT Perfusion		
	Base	Cerebrum	Intracranial	Cervical	Protocol I	Protocol II	Protocol III
Collimation (mm)	20 × 1.2	20 × 1.2	64 × 0.6	64 × 0.6	20 × 1.2	20 × 1.2	20 × 1.2
Table feed (mm)	24	24	45.9	69.7	0	0	0
Pitch	1	1	1.2	1.8	0	0	0
Tube current (mAs <sub>eff</sub> )	350	300	160	115	270	200	200
Electrical mA	350	300	383	417	270	200	200
Potential (kV)	120	120	100	120	80	80	120
Rot. time (s)	1	1	0.5	0.33	1	1	1
Scan length (mm)	48	95	250	280	24	24	24
Scan time (s)			6.25	4.58	40	40	40
CTDI <sub>vol</sub> total (mGy)	39.86	34.16	12.79	7.9	432	320	970
DLP total (mGy × cm)	203	348	386	277	1037	768	2330

**Note:**—Table feed indicates table movement per second. Pitch corresponds to the dose-relevant pitch (table feed per total collimation considering the number of detector rows acquired simultaneously). CTDI indicates computed tomography dose index; DLP, dose-length product.

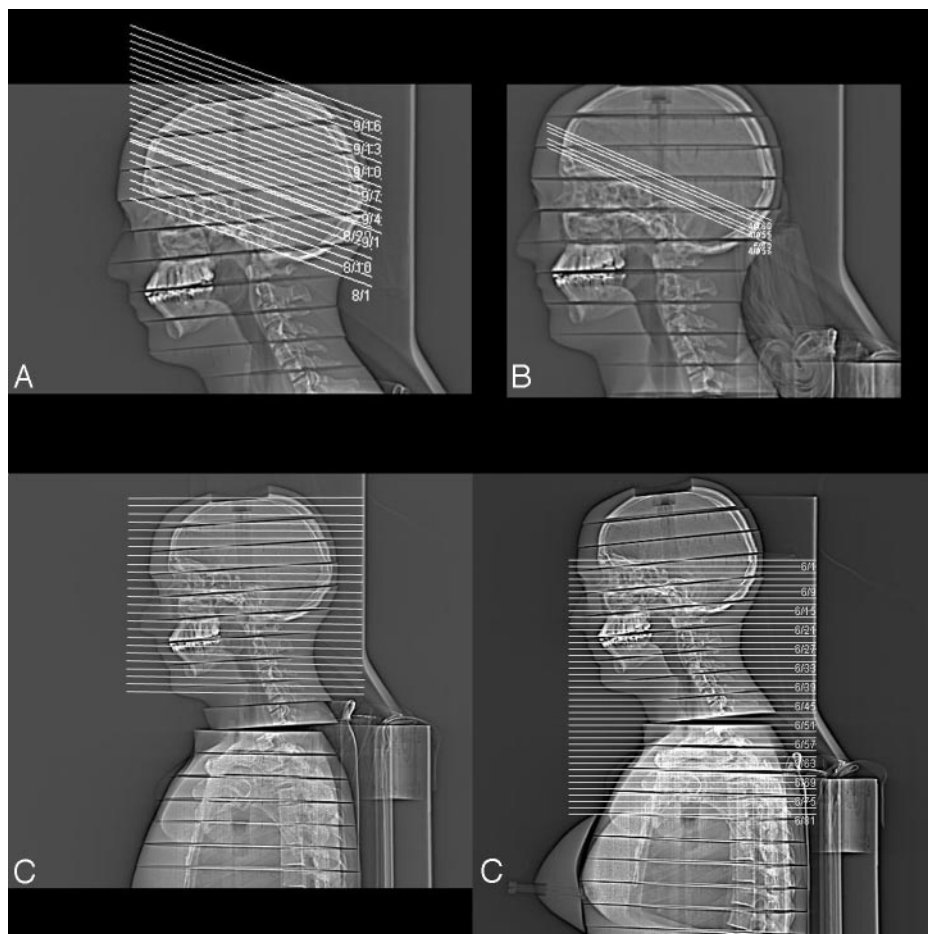


**Fig 1.** Topogram of Alderson-Rando-phantom demonstrating scan areas for standard CT of the head (A), CTP (B), as well as intracranial CTA (C), and cervical CTA (D), respectively.

were done as different organs and therefore organ doses are relevant.<sup>11</sup>

## Results

Standard CT protocols of the head showed a volume computed tomography dose index (CTDI<sub>vol</sub>) of 39.86 mGy, and a dose length product (DLP) of 203 mGy × cm, respectively, for the examination of the skull base and posterior fossa. Due to less extensive bone structure, supratentorial scanning is performed with lower tube current, resulting in a CTDI<sub>vol</sub> of 34.16 mGy and a DLP of 348 mGy × cm. The intracranial CTA as well as the CTA of the cervical vessels had lower CTDI<sub>vol</sub>. Because of the long examination area, DLP reached values between 277 and 386 mGy × cm.

Measurements using anthropomorphic phantoms allow for estimation of local organ doses. These are reported in detail in

Depending on the scan protocol the phantom was equipped with at least 40 TLDs, all relevant organs within the primary beam were covered with at least 2 TLDs representing the organ dose. In addition, particularly radiation sensitive organs like the ovaries or testes were included. Data from TLDs directly positioned within an organ (thyroid, gonads) were directly used to define the organ dose after addition of the measured values and division by the number of TLDs. For larger structures or organs (eg, lungs, liver, esophagus), the organ dose was defined as mean of at least 3 TLDs positioned in the region of this organ.

The total effective dose results from addition of the single organ doses after multiplication with the appropriate weighting factor (ICRP 60<sup>10</sup>). Separate calculations for male and female patients

Table 2. The total radiation dose of the brain was 22.2 mGy, whereas for the eye lenses and the thyroid, particularly sensitive organs, 5.4 and 1.1 mGy were noted. Both for the CTA of the intracranial as well as the cervical vessels these doses did not exceed 20 mGy. However, local exposure of the esophagus and the lungs was higher for the cervical CTA as these structures were partly located within the area of the primary beam.

The 3 simulated CTP protocols revealed local organ doses of the brain in the area of the primary beam ranging from 114.1 to 444.2 mGy as highest cerebral dose (Table 2). Calculations including measurements from LiF-TLD in the direct vicinity resulted in a total cerebral organ dose ranging from

**Table 2: Organ doses and effective doses as measured by lithium fluoride thermoluminescent dosimeters in several positions for different scan protocols**

	Standard CT	CT Angiography		CT Perfusion		
		Intracranial	Cervical	Protocol I	Protocol II	Protocol III
Organ doses (mGy)						
Cerebrum (overall)	22.2	11.7	9.8	117.9	82.5	325.2
Cerebrum (highest dose)	35.2	9.2	10.3	164.9	114.1	444.2
Skin (total)	11.7	3.1	0.7	26.9	20.2	126.9
Skin (highest dose)	36.2	16.1	19.2	112.3	87.2	404.8
Bone marrow (total)	2.2	2.7	4.3	4.2	4.2	20.7
Bone marrow (skull)	15.8	9.9	10	21.4	21.9	118.1
Eye lens	5.4	15.2	13	13.7	7.9	35.7
Thyroid	1.1	19.7	19.2	2.4	2.4	9.2
Esophagus	0.7	4.8	7.5	2.0	1.2	4.7
Lung	0.4	0.6	4.0	0.7	0.4	1.0
Gonads	0.2	0.3	0.2	0.2	0.2	0.2
Effective dose (mSv)*	1.7	1.9	2.8	1.2/1.3	1.1/1.2	5.0

\*Data for effective doses are given for male and female subjects if different (male/female).

82.5 to 325.3 mGy, with exposure of the eye lens reaching from 7.9 to 35.7 mGy. The area of the thyroid showed 2.4 to 9.2 mGy. Esophagus and lungs revealed a local dose of up to 4.7 and 1.0 mGy, respectively.

Dose measurements assessing exposure of the bone marrow (2.2 mGy for standard CT and 20.7 mGy for CTP protocol III) and the skin (0.7 mGy for cervical CTA up to 126.9 mGy in CTP protocol III) reflect approximate organ doses as these data result from LiF-TLD, which were both positioned within the area of the primary beam and in areas exposed to scatter radiation only. Regarding only LiF-TLD in the directly exposed area, local doses between 9.9 and 118.1 mGy (bone marrow) as well as 9.2 and 444.2 mGy (skin) were seen.

The effective doses of the CT protocols examined in the present study are given in detail in Table 2. Effective doses for standard CT as well as the 2 CTA protocols ranged between 1.7 and 2.8 mSv without a conceivable sex difference. For the 3 CTP protocols, slight differences for male and female subjects were found; however, only the third protocol had higher values of 5 mSv.

## Conclusions

Imaging studies assessing cerebral perfusion have become an essential part in the early evaluation of patients with acute cerebral ischemia.<sup>1,3,12</sup> However, diffusion and perfusion MR imaging has limited accessibility and implies several contraindications like implanted pacemakers.<sup>2</sup> Lately, stroke imaging has become available using not only MR imaging but also CT.<sup>6,13,14</sup> Many institutions can offer CT imaging without a long time delay after symptom onset so that modern concepts depending on early diagnosis within the narrow therapeutic “window” may profit from comprehensive CT stroke imaging.<sup>15</sup>

Although the MDCT scanner offers fast and reliable stroke imaging, the main disadvantage of a limited coverage of CTP concentrated mainly on the level of the basal ganglia has to be mentioned, including the impossibility to assess early cytotoxic edema.<sup>3</sup> Furthermore, first clinical reports hint at possible adverse effects of CTP examinations; visible hair loss was documented in 3 patients who underwent CTP studies.<sup>8</sup> This study estimated local doses due to MDCT of the head, includ-

ing perfusion studies as well as cerebral angiography within the range of 1 to 3 Gy as the likely cause of temporal hair loss.

In a review on cerebral CTP, estimations of local doses based on Monte Carlo methods were published; effective doses between 2.0 and 3.4 mSv for the perfusion study and between 1.5 and 2.5 mSv for the routine brain study were estimated. The actual dose to the irradiated volume was discussed to range between 110 and 300 mGy.<sup>6,16</sup>

The present study with data based on phantom measurements supports these calculations, including standard CT of the head, CTP, and CTA of intracranial as well as cervical vessels using MDCT. Local doses within the area of the primary beam may reach 137–495 mGy, whereas total organ dose of the brain may result in 110–350 mGy. For the eye lenses and for the thyroid, 26–56 and 23–30 mGy were measured, respectively. Comparable data were found for the bone marrow of the skull and the skin. Effective doses for the combination of all 3 studies may range between 4.7 and 9.5 mSv.

For cerebral CTP, few data exist on direct measurements both on local organ doses that have to be expected in the area of the primary beam as well as on the effective dose as an indicator of the general radiation exposure of the patient.<sup>7</sup> A dedicated analysis on central and peripheral dose values showed the direct dependence of doses on the chosen examination parameters. This study demonstrated local doses between 90 and 1600 mGy in the center as well as a range from 160 to 2260 mGy on the surface of the head phantom.<sup>7</sup> Although in the present study, partly comparable scanning parameters were chosen (eg, 80 kV/200 mA; 120 kV/200 mA), data differ considerably. The longer examination time of 60 seconds in the study of Hirata et al<sup>7</sup> leads to a linear increase in dose by a factor of 1.5. Even when this is taken into consideration, local cerebral doses in the present study are lower by a factor of 2. Although this may be partly attributable to the different types of scanners (4-detector-row versus 64-detector-row), including the scanner geometry and beam filter, other factors may play a role. In the present study, LiF-TLD were used to assess radiation dose. The type of TLD used in the previous work was not stated. Therefore, more sensitive TLD (eg, calcium-fluoride) may have been used and may lead to



higher dose values. Furthermore, a response variation of up to 15% using TLD for measuring dose can occur.<sup>17</sup>

Different scan protocols have been evaluated in the present study, because various scanning protocol designs have been published.<sup>3,4,6,18-21</sup> In particular, alterations of the tube potential have the opportunity to reduce patients' exposure combined with the theoretic advantage of increased conspicuity of contrast media.<sup>20</sup> The postulated decrease in dose (by a factor of 2.8) could be proved in the present study, in that the local dose of the cerebrum was lowered from 325 to 82 mGy. Other organs or areas showed the same dose reduction. Effective dose was reduced from 5 to 1.1 mSv (male) or 1.2 mSv (female). This dependence of local and effective doses on varying scan parameters demonstrates the need for further studies concerning image quality required for perfusion analysis. Another possible way of lowering patients' exposure in CTP would be to reduce the number of scans per time; however, further work is warranted to define the lowest sampling rate necessary.<sup>5,22</sup>

Dose measurements in standard CT of the head have been published previously for single-section sequential or spiral CT scanner. These data range between 0.5 and 5 mSv depending on technical factors as well as the age of the patients.<sup>23-30</sup> Local doses of the brain parenchyma were reported to be below 100 mGy.<sup>26,27</sup> Although a MDCT was used in the present study, an increase of the effective dose compared with previous data was not noted. These dose values all fulfill both the German as well as the European Guidelines on Quality Criteria for Computed Tomography.<sup>31,32</sup>

The biologic effects of low-dose radiation of a circumscribed volume of cerebral parenchyma are not well understood. Lately, significant deficits in cognitive function were described in children exposed to low-dose brain irradiation (eg, 250 mGy) for the treatment of cutaneous hemangioma.<sup>33</sup> Although this may be true for the developing brain, most patients undergoing stroke imaging are adults with microvascular or macrovascular disease or other entities that may add to loss of cognitive function. The benefit of comprehensive imaging in the clinical situation of acute stroke, aiming at early and specific therapy, however, can outweigh the potential radiation risk. This is particularly true in view of contraindications to MR imaging including pacemakers or claustrophobia. However, further clinical trials are needed to prove the benefit of MDCT stroke imaging in terms of an improved clinical outcome.

Direct radiation effects concerning the eye lenses or the thyroid gland were documented at higher doses both regarding single and repeated irradiation. The most likely result may be cataract formation and the development of thyroid malignancy.<sup>34-36</sup> However, the minimal doses required to increase cancer risk remain unclear.<sup>37,38</sup> Cataract formation is believed not to occur with doses lower than 1–2 Gy for a single exposure.<sup>39</sup> However, lenticular punctate calcifications and vacuoles have been observed long-term after exposure to 100 mGy during childhood.<sup>40</sup> For the population in question, undergoing stroke imaging using CT, these risks may not become clinically relevant.

To date, no data exist with respect to CTA of the cervical or intracranial vessels using MDCT. In the present study, CTA of cerebral and cervical vessels did not show particular differ-

ences in terms of effective doses. Local organ doses were different in that esophagus and lungs showed higher values for cervical MDCTA, because this examination was extended down to the aortic arch to demonstrate possible pathologic conditions in that area.

## Summary

Comprehensive stroke imaging using CT may lead to effective doses in the range of 5–10 mSv, depending on the chosen scan parameters. Local doses do not reach thresholds for the development of cataract formation, induction of thyroid malignancy, or hair loss. Therefore, the patient population undergoing stroke imaging using MDCT—including patients with contraindications to MR imaging—may benefit from early therapy based on imaging findings. Economic issues and availability are in favor of CT stroke imaging. Further developments including reduced tube current and potential as well as a reduced number of scans over time may lead to a decrease in dose. However, limited coverage of CT perfusion studies, the impossibility of delineating early cytotoxic edema, and radiation exposure, particularly in case of repeated examinations, should alert physicians to reflect on which method may be more adequate for patients with acute stroke.

## References

1. Neumann-Haefelin T, Wittsack HJ, Wenserski F, et al. **Diffusion- and perfusion-weighted MRI. The DWI/PWI mismatch region in acute stroke.** *Stroke* 1999;30:1591–97
2. Singer OC, Sitzer M, du Mesnil de Rochemont R, et al. **Practical limitations of acute stroke MRI due to patient-related problems.** *Neurology* 2004;62:1848–49
3. Miles KA. **Brain perfusion: computed tomography applications.** *Neuroradiology* 2004;46 Suppl 2:S194–200
4. Kloska SP, Nabavi DG, Gaus C, et al. **Acute stroke assessment with CT: do we need multimodal evaluation?** *Radiology* 2004;233:79–86
5. Wintermark M, Smith WS, Ko NU, et al. **Dynamic perfusion CT: optimizing the temporal resolution and contrast volume for calculation of perfusion CT parameters in stroke patients.** *AJNR Am J Neuroradiol* 2004;25:720–29
6. Hoeffner EG, Case I, Jain R, et al. **Cerebral perfusion CT: technique and clinical applications.** *Radiology* 2004;231:632–44
7. Hirata M, Sugawara Y, Fukutomi Y, et al. **Measurement of radiation dose in cerebral CT perfusion study.** *Radiat Med* 2005;23:97–103
8. Imanishi Y, Fukui A, Niimi H, et al. **Radiation-induced temporary hair loss as a radiation damage only occurring in patients who had the combination of MDCT and DSA.** *Eur Radiol* 2005;15:41–46
9. ICRP. **Reference man: anatomic, physiological and metabolic characteristics.** Publication 23. Oxford, UK: Pergamon Press; 1975
10. ICRP. **1990 Recommendation of the International Commission on Radiological Protection.** ICRP publication no. 60. Oxford, UK: Pergamon Press; 1991
11. McCollough CH, Schueler BA. **Calculation of effective dose.** *Med Phys* 2000;27:828–37
12. Thomalla GJ, Kucinski T, Schoder V, et al. **Prediction of malignant middle cerebral artery infarction by early perfusion- and diffusion-weighted magnetic resonance imaging.** *Stroke* 2003;34:1892–99
13. Bohner G, Forschler A, Hamm B, et al. **Quantitative perfusion imaging by multi-slice CT in stroke patients.** *Fortschr Röntgenstr* 2003;175:806–13
14. Koenig M, Kraus M, Theek C, et al. **Quantitative assessment of the ischemic brain by means of perfusion-related parameters derived from perfusion CT.** *Stroke* 2001;32:431–37
15. Lev MH, Nichols SJ. **Computed tomographic angiography and computed tomographic perfusion imaging of hyperacute stroke.** *Top Magn Reson Imaging* 2000;11:273–87
16. Frey GD, Rumboldt Z. **Radiation effects from perfusion CT.** *Radiology* 2005;234:638; author reply 638
17. Fairbanks EJ, DeWerd LA. **Thermoluminescent characteristics of LiF:Mg,Ti from three manufacturers.** *Med Phys* 1993;20:729–31
18. Klingebiel R, Bohner G, Zimmer C, et al. **Using multislice spiral CT in neuro-radiologic imaging.** *Nervenarzt* 2002;73:729–35
19. Koenig M, Klotz E, Luka B, et al. **Perfusion CT of the brain: diagnostic approach for early detection of ischemic stroke.** *Radiology* 1998;209:85–93
20. Wintermark M, Maeder P, Verduin FR, et al. **Using 80 kVp versus 120 kVp in**

- perfusion CT measurement of regional cerebral blood flow. *AJNR Am J Neuroradiol* 2000;21:1881–84
21. Schramm P, Schellinger PD, Klotz E, et al. Comparison of perfusion computed tomography and computed tomography angiography source images with perfusion-weighted imaging and diffusion-weighted imaging in patients with acute stroke of less than 6 hours' duration. *Stroke* 2004;35:1652–58
  22. Hirata M, Murase K, Sugawara Y, et al. A method for reducing radiation dose in cerebral CT perfusion study with variable scan schedule. *Radiat Med* 2005;23:162–69
  23. Brix G, Nagel HD, Stamm G, et al. Radiation exposure in multi-slice versus single-slice spiral CT: results of a nationwide survey. *Eur Radiol* 2003;13:1979–91
  24. Cohnen M, Fischer H, Hamacher J, et al. CT of the head by use of reduced current and kilovoltage: relationship between image quality and dose reduction. *AJNR Am J Neuroradiol* 2000;21:1654–60
  25. Conway BJ, McCrohan JL, Antonsen RG, et al. Average radiation dose in standard CT examinations of the head: results of the 1990 NEXT survey. *Radiology* 1992;184:135–40
  26. Huda W, Chamberlain CC, Rosenbaum AE, et al. Radiation doses to infants and adults undergoing head CT examinations. *Med Phys* 2001;28:393–99
  27. Huda W, Lieberman KA, Chang J, et al. Patient size and x-ray technique factors in head computed tomography examinations. I. Radiation doses. *Med Phys* 2004;31:588–94
  28. McCrohan JL, Patterson JF, Gagne RM, et al. Average radiation doses in a standard head examination for 250 CT systems. *Radiology* 1987;163:263–68
  29. Smith A, Shah GA, Kron T. Variation of patient dose in head CT. *Br J Radiol* 1998;71:1296–301
  30. Nagel H-D, Galanski M, Hidajat N, et al. *Radiation exposure in computed tomography—fundamentals, influencing parameters, dose assessment, optimization, scanner data, terminology*. Frankfurt: COCIR; 2000
  31. Bundesärztekammer. Leitlinie der Bundesärztekammer zur Qualitätssicherung in der Computertomographie. *Dt Arztebl* 1992;89:C2368
  32. Communities CotE. *European Guidelines on Quality Criteria for Computed Tomography, Report EUR 16262 EN 1999*. Available at <http://www.drs.dk/guidelines/ct/quality/htmlindex.htm3/11/2004>. 1999
  33. Hall P, Adami HO, Trichopoulos D, et al. Effect of low doses of ionising radiation in infancy on cognitive function in adulthood: Swedish population based cohort study. *BMJ* 2004;328:19
  34. Ehemann CR, Garbe P, Tuttle RM. Autoimmune thyroid disease associated with environmental thyroidal irradiation. *Thyroid* 2003;13:453–64
  35. Merriam GR, Jr., Focht EF, Parsons RW. The relative radiosensitivity of the young and the adult lens. *Radiology* 1969;92:1114
  36. Ron E, Lubin JH, Shore RE, et al. Thyroid cancer after exposure to external radiation: a pooled analysis of seven studies. *Radiat Res* 1995;141:259–77
  37. Brenner DJ, Doll R, Goodhead DT, et al. Cancer risks attributable to low doses of ionizing radiation: assessing what we really know. *Proc Natl Acad Sci U S A* 2003;100:13761–66
  38. Cohen BL. Cancer risk from low-level radiation. *AJR Am J Roentgenol* 2002;179:1137–43
  39. Henk JM, Whitelocke RA, Warrington AP, et al. Radiation dose to the lens and cataract formation. *Int J Radiat Oncol Biol Phys* 1993;25:815–20
  40. Wilde G, Sjostrand J. A clinical study of radiation cataract formation in adult life following gamma irradiation of the lens in early childhood. *Br J Ophthalmol* 1997;81:261–66